FARADAY

Rotational energy transfer and rotationally specific vibration–vibration intradyad transfer in collisions of C_2H_2 $\tilde{X}\,^1\Sigma_g^+(3_1/2_1 4_1 5_1, J = 10)$ with C_2H_2, Ar, He and H_2†

Sarah Henton, Meezanul Islam, Simon Gatenby‡ and Ian W. M. Smith*

School of Chemistry, The University of Birmingham, Edgbaston, Birmingham, UK B15 2TT. E-mail: i.w.m.smith@bham.ac.uk

Received 28th July 1998, Accepted 19th August 1998

Infrared–ultraviolet double resonance (IRUVDR) experiments have been performed on samples of pure C_2H_2 and on C_2H_2 diluted in Ar, He and H_2. Pulses of tunable IR radiation from an optical parametric oscillator (OPO) excited molecules of C_2H_2 to the $J = 10$ rotational level of the lower component state (II) of the $(3_1/2_1 4_1 5_1)_{II}$ Fermi dyad in the $\tilde{X}\,^1\Sigma_g^+$ electronic ground state of C_2H_2 and tunable UV radiation was used to record laser-induced spectra at short delays. In this way, state-to-state rate coefficients have been determined for two kinds of processes:§ (a) rotational energy transfer (RET) induced by collisions with C_2H_2, Ar, He and H_2 from the initial level $J_i = 10$ to other levels ($J_f = 2$–8, 12–20) within the same component (II) of the $(3_1/2_1 4_1 5_1)$ Fermi dyad, and (b) intradyad transfer in C_2H_2–C_2H_2 collisions to specific levels ($J_f = 2$–14, 18) in the other component (I) of this Fermi dyad. Transfer from II to I is found to account for *ca.* 16% of the total relaxation from (II, $J_i = 10$). The distribution of state-to-state rate coefficients for RET becomes broader as the mass of the collision partner increases, in accord with the predictions of a simple classical model. Absolute values of the state-to-state rate coefficients are determined by scaling the results to the previously determined rate coefficients for rotational relaxation by the same collision partner. It is suggested that intradyad transfer is relatively facile because of the difference in the two diagonal terms in the vibrational matrix element for the transition, with the $\langle 2_1 4_1 5_1 | V | 2_1 4_1 5_1 \rangle$ component being larger than the $\langle 3_1 | V | 3_1 \rangle$ component.

In the Introduction to the preceding paper,[1] referred to here as Part I, we have emphasised the unique spectroscopic and dynamical character of C_2H_2 which makes it the target of a range of interesting questions concerning both its unimolecular and its collisional dynamics. In many recent experiments, double resonance (DR) techniques have been exploited to examine both vibrational[1–9] and rotational energy transfer[5–15] in collisional processes involving C_2H_2. In such experiments, molecules of C_2H_2 are promoted to a specific rovibrational level in the $\tilde{X}\,^1\Sigma_g^+$ electronic ground state using IR, visible or stimulated Raman excitation, and the evolution of this sub-set of molecules is observed using a tunable UV laser to generate laser-induced fluorescence (LIF) *via* the $\tilde{A}\,^1A_u$ excited state.

Although they lead to considerable spectroscopic complexity, the extensive perturbations in the vibrational manifolds of both the $\tilde{X}\,^1\Sigma_g^+$ [16–20] and $\tilde{A}\,^1A_u$ [21] electronic states do facilitate infrared–ultraviolet double resonance (IRUVDR) experiments on C_2H_2. Thus the experiments reported in Part I and in this paper report measurements on the two lowest lying Fermi dyads, $(3_1/2_1 4_1 5_1)_{I,II}$ and $(3_1 4_1/2_1 4_2 5_1)_{I,II}$.¶ Even in the lower of these two dyads, the mixing between the zero order states $|3_1\rangle$ and $|2_1(4_1 5_1)^0\rangle$ is complete, *i.e.* the mixing coefficients associated with these zero order states in the expressions for eigenstates I and II are essentially equal in magnitude (see Table 1 in Part I [1]). From an experimental point of view, this means that both components of the dyad share the IR activity associated with the $|3_1\rangle$ fundamental. In addition, the presence of excitations in the ν_2 and ν_4 modes enhances the strength of bands in the $\tilde{A}\,^1A_u$–$\tilde{X}\,^1\Sigma_g^+$ system, because of the change to a *trans*-bent structure with a longer C—C bond which occurs on electronic excitation.[1] These factors have also assisted work on other higher rovibrational levels in $C_2H_2(\tilde{X}\,^1\Sigma_g^+)$.

As well as these practical considerations, the existence of strong Fermi resonances between vibrational levels in the electronic ground state of C_2H_2 confers special interest on studies of the dynamics of this molecule, and its behaviour serves as a bridge between those expected for diatomic and large polyatomic molecules. In particular, it allows one to investigate how energy transfer processes both within a Fermi dyad and from a Fermi dyad are affected by the existence of the resonance.

In Part I,[1] we reported rate coefficients for two kinds of processes involving the $(3_1/2_1 4_1 5_1)_{I,II}$ and $(3_1 4_1/2_1 4_2 5_1)_{I,II}$ dyads: (a) transfer between the two component states of each Fermi dyad induced by collisions with C_2H_2, N_2 and H_2 under rotationally equilibrated conditions, and (b) vibrational relaxation from each coupled pair of Fermi dyad states in collisions with the same gases. In the present paper, we report rate coefficients for two processes within the $(3_1/2_1 4_1 5_1)_{I,II}$ dyad: (a) rotational energy transfer (RET) induced by collisions with C_2H_2, Ar, He and H_2 from $J_i = 10$ to other levels ($J_f = 2$–8, 12–20) within the same component (II) of this dyad, and (b) rotationally specific vibration–vibration (V–V) intradyad transfer in C_2H_2–C_2H_2 collisions from the same

† The notation for vibrational states is explained in the first footnote to the preceding paper, referred to hereafter as Part I.[1]

‡ Present address: Physical and Theoretical Chemistry Laboratory, South Parks Road, Oxford, UK OX1 3QZ.

§ Part I also describes measurements of rate coefficients for two kinds of process induced by collisions with C_2H_2, N_2 and H_2: (a) transfer between states in the $(3_1/2_1 4_1 5_1)$ and $(3_1 4_1/2_1 4_2 5_1)$ dyads; (b) vibrational relaxation from these dyad states.

¶ Strictly the states identified here are part of larger polyads. However, at these relatively low levels of excitation, the mixing between members of the polyads are limited. Further discussion of this point is given in the Introduction to Part I.

initial J level in state II to levels (J_f = 2–14, 18) in component I of this Fermi dyad. The $(3_1/2_1 4_1 5_1)_{I,II}$ dyad is of particular interest because detailed characterisation of these states by Vander Auwera *et al.*[17] has revealed the J-dependent nature of the coupling.

A large number of studies on RET in diatomic species has been reported.[22–28] Also RET in a range of polar polyatomic molecules, in addition to C_2H_2, have been investigated: for example, NH_3,[29] CH_3OH,[30] C_2H_5OH [31] and HCN.[32] However, rate measurements have often been restricted to self-relaxation and state-to-state rotational transfer in polyatomic molecules induced by foreign collision partners has not been thoroughly explored. This has certainly been the case for acetylene.[4–14] From a theoretical viewpoint, collisions between molecules and rare gas atoms are far more tractable so such investigations are desirable. Frost[11] reported some results on state-to-state rotational energy transfer in the $(3_1/2_1 4_1 5_1)$ dyad of C_2H_2 induced by collisions with argon. The present work is a comprehensive extension of that preliminary study, with He and H_2 chosen as collision partners in addition to Ar. A limited number of state-to-state rate constants have also been determined by Tobiason *et al.*[9] for rotational relaxation of C_2H_2 by argon within the 3_3 manifold. Theoretical models may more easily be applied to such molecule–atom systems, and even full quantum calculations have been performed for comparison with experiment in the case of NO.[28b]

Experimental method and procedures

The apparatus and experimental procedures were similar to those used in previous IRUVDR experiments on acetylene performed in this laboratory including those described in Part I.[1–3,10,11] Consequently, only a very brief description will be given here, emphasising aspects which are peculiar to the present set of experiments.

In all the experiments reported in the present paper, C_2H_2 molecules were excited by direct IR absorption to the J = 10 level of the $(3_1/2_1 4_1 5_1)_{II}$ state. Tunable IR radiation was provided by an optical parametric oscillator (OPO) which was pumped by the fundamental 1.064 (μm output from a Nd:YAG laser (Spectron SL800). The output of the OPO at *ca.* 3300 cm^{-1} was tuned to a line in the $(3_1/2_1 4_1 5_1)_{II} \leftarrow 0$ IR band of C_2H_2 with the aid of a spectrophone containing 100 Torr of C_2H_2. UV probe radiation at *ca.* 246 nm was provided by the frequency doubled output from a XeCl excimer (Lambda Physik 110 series) pumped dye laser (Lambda Physik FL2002). The pump and probe laser beams counter-propagated through a simple cell equipped with appropriate windows. The arrangements for collecting and processing the observed LIF signals were as given previously.[1–3,10,11]

In each of the present experiments, the delay between the pump and probe lasers was fixed and the frequency of the UV probe laser was scanned to record a LIF spectrum of the $\tilde{A}\,^1A_u(3_1 4_1/3_1 6_1)$–$\tilde{X}\,^1\Sigma_g^+(3_1/2_1 4_1 5_1)_{I,II}$ band. The spectroscopy of this band is complex due to the Coriolis coupling between the $\tilde{A}(\nu_4)$ and $\tilde{A}(\nu_6)$ vibrations.[21] Assignments for progressions within this band have been obtained which essentially agree with earlier work in this laboratory.[11] This spectroscopic work is described in the next section.

The C_2H_2 used in these experiments was provided by BOC (Industrial Grade). It was purified by several freeze–pump–thaw cycles. Ar, He and H_2 were taken from cylinders and stored in Pyrex bulbs fitted with a cold finger immersed in liquid N_2 before use. All measurements were made at room temperature (295 ± 5 K).

Spectroscopic aspects

In order to assign lines in the $\tilde{A}\,^1A_u(3_1 4_1/3_1 6_1)$–$\tilde{X}\,^1\Sigma_g^+(3_1/2_1 4_1 5_1)_{I,II}$ bands, many LIF spectra were collected,

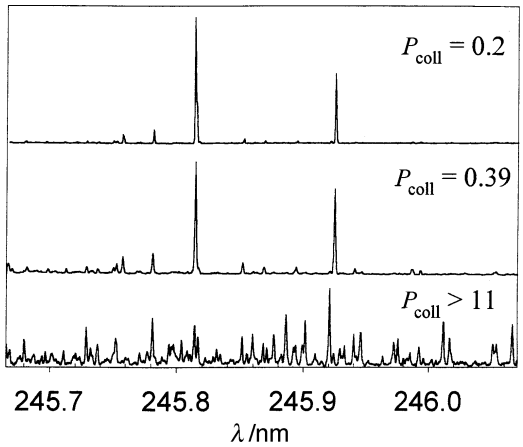

Fig. 1 Examples of double resonance spectra recorded at different delays between the IR pump and UV probe laser. In this example, the level J = 10 in the $\tilde{X}(3_1/2_1 4_1 5_1)_I$ vibrational state is populated by IR absorption in a sample of pure C_2H_2 and gives rise to the strong lines in the first two spectra. The UV probe laser is scanned through part of the $\tilde{A}(3_1 4_1/3_1 6_1) \leftarrow \tilde{X}(3_1/2_1 4_1 5_1)_I$ band. Different delay times are recorded as P_{coll}, the fraction of the average time between collisions. The last spectra is similar to those used to determine line intensities.

at various pump–probe delays, following excitation of C_2H_2 to selected rotational levels within the $(3_1/2_1 4_1 5_1)_{I,II}$ Fermi dyad states. A series of such spectra is shown in Fig. 1. The calibration of the IR laser source was not sufficiently good to be sure which rovibrational level was excited in any given experiment, making the assignment of lines in the UV spectrum more difficult. Trial assignments were made following the collection of a large number of spectra. Then reduced term values for each transition were calculated using the procedure employed by Utz *et al.*[21] These quantities are defined by the expression

$$T_{red} = \nu_{LIF} + (E_{v''J''}/hc) - T_0 - (B_{av}J'(J'+1)/hc) \quad (1)$$

where ν_{LIF} is the wavenumber of a line in the LIF spectrum, $E_{v''J''}$ is the energy of the rovibrational state in $\tilde{X}\,^1\Sigma_g^+$ from which molecules are excited, T_0 is the electronic band origin (42 198 cm^{-1} [33]), B_{av} is set equal to $(B + C)/2$, *i.e.* the mean of the two smallest rotational constants of $C_2H_2(\tilde{A}\,^1A_u)$, and J' is the rotational quantum number of the upper state. (The electronically excited $\tilde{A}\,^1A_u$ state of acetylene is very close to being a prolate asymmetric top.[21])

A plot of T_{red} *versus* $J'(J'+1)$ derived from such experiments is shown in Fig. 2. Using such a plot, incorrect assignments could be easily identified. Also included on this plot are

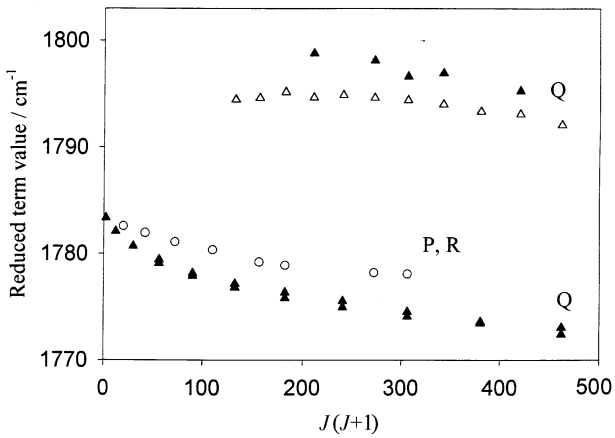

Fig. 2 Reduced term value plot derived for the $\tilde{A}(3_1 4_1/3_1 6_1)$ pair of states. Hollow symbols indicate e parity levels, solid symbols indicate f parity. Q-branch (▲) and P-, R-branch (○) transitions from $\tilde{X}(3_1/2_1 4_1 5_1)_{I,II}$. Q-branch (△) transitions assigned from $\tilde{X}(3_1 4_1/2_1 4_2 5_1)_{II}$.

Table 1 Zero-order identity and approximate spectroscopic constants for $\tilde{A}(3_1 4_1/3_1 6_1)$ vibrational levels

ν_{obs}/cm^{-1}	$[(B+C)/2]/cm^{-1}$	Vibrational state	K_a
1784	1.05	$3_1 4_1$	1
1792	1.06	$3_1 4_1$	0
≈1798	≈1.05	$3_1 6_1$	0

data obtained following excitation to the $\tilde{X}(3_1 4_1/2_1 4_2 5_1)$ dyad (these states are otherwise not relevant to this work). The correct assignment results in the smooth, nearly horizontal, lines that are shown in Fig. 2.

Because parity selection rules are strictly obeyed and R-branch IR transitions are used to access levels in the $(3_1/2_1 4_1 5_1)_{I,II}$ dyad, which is of σ^+ character, the J levels which are populated must be of e parity. Each K_a sub-band extends to a minimum value of $J = K_a$ but insufficient spectra have been collected to make an unambiguous assignment of the observed K_a sub-bands. These findings may be compared to those of Utz *et al.*[21] for the $(4_1/6_1)$ dyad levels in the $\tilde{A}\,^1A_u$ state, as the extent of the Coriolis mixing is likely to be very similar in these two sets of levels. This similarity is evident if one inspects Fig. 4 of ref. 21(*a*). Assignments of the K_a sub-bands are therefore tentatively suggested in Table 1. The sub-bands which give rise to the reduced term values in the range from *ca.* 1784–1798 cm^{-1} are apparently those observed by Frost.[11] In the course of our experiments it was found necessary to find alternative means to monitor the populations of $J_I = 10$ and $J_{II} = 14$, due to the near coincidence of lines from these levels in the Q-branch of the $\tilde{A}\,^1A_u(3_1 4_1/3_1 6_1)$–$\tilde{X}\,^1\Sigma_g^+(3_1/2_1 4_1 5_1)_{I,II}$ bands [the subscripts I and II attached to J refer to the upper and lower component states of the $(3_1/2_1 4_1 5_1)_{I,II}$ dyad, respectively]. The alternative lines used to estimate populations in these levels are shown in Fig. 3.

The second major aim in these spectroscopic experiments was to determine appropriate intensity factors so as to be able to convert measured line intensities to populations in the absorbing levels in the $(3_1/2_1 4_1 5_1)$ dyad. A number of spectroscopic properties of the $\tilde{A}\,^1A_u$ and $\tilde{X}\,^1\Sigma_g^+$ states in C_2H_2 make it necessary to determine these factors experimentally, rather than calculate them. These properties include the mixing of σ and δ character in the $\tilde{X}$ state dyad,[17] axis-switching in the $\tilde{A}\,^1A_u$–$\tilde{X}\,^1\Sigma_g^+$ transition, and the strength of Coriolis interactions in the $\tilde{A}\,^1A_u$ state. The intensity factors were obtained by collecting LIF spectra under conditions

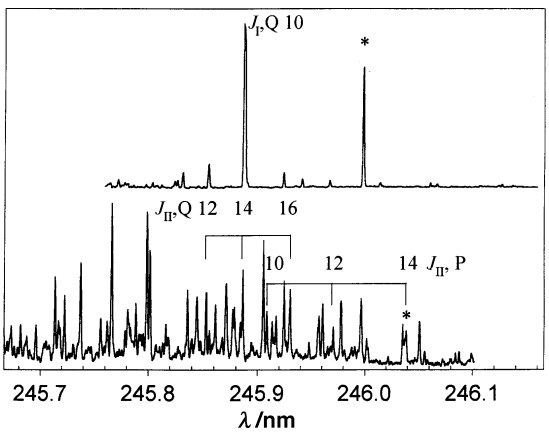

Fig. 3 Spectra showing the alternative lines (*) used to monitor population in $J_I = 10$ and $J_{II} = 14$. The former, in the upper panel, using a line from an unassigned K_a sub-band, as the P- and R-branch transitions of the assigned sub-band lie outside the range used. $J_{II} = 14$, lower panel, is monitored using the corresponding P-branch transition.

where rotational relaxation would be complete. Then they could be found by comparing the measured line intensities with the corresponding Boltzmann populations. The intensity factors determined in this way have been deposited as Supplementary Data.‖

Results and discussion

The results presented for self-relaxation and for relaxation by foreign collision partners are essentially independent of one another so these results are presented and discussed below in separate sections. However, the general strategy was common to both sets of experiments, so it is outlined first.

LIF spectra were recorded at fixed time delays between the pulses from the IR pump and UV probe lasers. This delay (δt) was set to correspond to a fraction ($P \leqslant 0.2$) of the total rotational relaxation time in the gas sample under investigation. In calculating P, we used the rate coefficients for total rotational relaxation (k_{rel}^M) determined by Frost and Smith[10] and the formula: $P = \sum_M k_{rel}^M[M]\ \delta t$, where k_{rel}^M is the rate coefficient for total relaxation of C_2H_2 in collisions with M. The aim was to convert the line intensities observed in these spectra to relative populations in individual J_f levels using the intensity factors determined earlier and listed in the Supplementary material.

The populations (N_f) for levels other than $J_{II} = 10$, which was directly populated by absorption of IR radiation, were assumed to arise as a result of collisons of molecules in the initially prepared state with C_2H_2 and, where appropriate, with M. This situation is represented approximately by the rate equation:[27b,28]

$$N_f(\delta t) = N_i(t=0)(k_{if}^{C_2H_2}[C_2H_2] + k_{if}^M[M])\ \delta t \qquad (2)$$

where $N_f(\delta t)$ is the population in level f at time delay δt and $N_i(t=0)$ is the population in the initally prepared state at zero time. Relative values of $(k_{if}^{C_2H_2}[C_2H_2] + k_{if}^M[M])$ for different final states f were determined from the relative intensities of lines from these different states in the LIF spectrum. The relative first-order rate coefficients were converted to absolute values using the rate coefficients for total relaxation by C_2H_2 and M[10] and the concentrations of the gases in the sample, with allowance made for vibrational relaxation.[1,34] To derive values of k_{if}^M from experiments on mixtures of C_2H_2 with M, it was necessary to correct for the contribution of self-relaxation using the state-to-state rate constants determined from experiments on samples of pure C_2H_2.

Of course, at the short delay times used in these experiments, most of the population remained in the initially prepared state. Since the PMT detector did not respond linearly to the wide range of LIF intensities from different lines, it was decided to use the present measurements to determine only the relative populations in the levels $J_f \neq J_i$ and hence to determine relative values of the state-to-state rate coefficients for transfer from J_i to J_f. These rate coefficients were then converted to absolute values using the established values of the rate coefficients for total removal by M from a specified initial J level.[10]

(a) Rotational energy transfer and rotationally specific V–V intradyad transfer in C_2H_2–C_2H_2 collisions: Results

To determine state-to-state rate coefficients for transfer from the initial state, $J_{II} = 10$, in C_2H_2–C_2H_2 collisions, LIF spectra were recorded at short delays ($\delta t \approx 100$ ns) from samples of *ca.* 100 mTorr of pure C_2H_2. Relative values of these rate coefficients were then derived from the relative intensities of lines in the spectra *via* the methods described in the previous section. The sum of these relative state-to-state

‖ Supplementary data (**SUP 57432**, 4 pp.) deposited with the British Library. Details are available from the Editorial Office.

Table 2 Experimental state-to-state rate coefficients (k_{if}), and the values for the reverse processes (k_{fi}) for transfer from and to the $\tilde{X}(3_1/2_1 4_1 5_1)_{II}$, $J = 10$ of C_2H_2 (units: 10^{-11} cm^3 molecule^{-1} s^{-1})

	RET		Intradyad	
J	k_{if}	k_{fi}	k_{if}	k_{fi}
2	2.7 ± 0.7[a]	6.4 ± 0.9		
4	3.2 ± 1.0	5.2 ± 1.2		
6	$7.5_5 \pm 1.0$	8.3 ± 1.2	$1.3_5 \pm 0.5$	1.5 ± 0.6
8	$27._8 \pm 3.1$	$27._6 \pm 3.1$	2.1 ± 0.5	2.1 ± 0.6
10	—	—	3.1 ± 1.4	3.4 ± 1.5
12	$17._4 \pm 2.2$	$19._8 \pm 2.5$	1.9 ± 0.7	$2.1_5 \pm 0.9$
14	5.5 ± 1.1	$7.0_5 \pm 1.5$	1.8 ± 0.7	$2.4_5 \pm 0.9$
16	2.7 ± 0.6	4.3 ± 0.9	—	—
18	1.6 ± 0.4	3.4 ± 0.9	$0.9_5 \pm 0.4$	$2.1_5 \pm 0.9$
20	1.0 ± 0.3	3.1 ± 0.9	—	—
Total	$69._4$		$11._3$	

[a] Cited uncertainty corresponds to 2σ error.

rate coefficients, including a statistical estimate of transfer to unobserved rotational levels and including an allowance for vibrational relaxation, was assumed to equal the value of 9×10^{-10} cm^3 molecule^{-1} s^{-1} which has been measured previously to be the rate coefficient for total removal from rovibrational levels in the $\tilde{X}\,^1\Sigma_g^+$ state of acetylene in self-collisons.[2,10,11,34] This procedure yielded the values for the state-to-state rate coefficients given in Table 2.

The sum of the state-to-state rate coefficients for intradyad transfer from $(3_1/2_1 4_1 5_1)_{II}$, $J = 10$ to observed rotational levels in $(3_1/2_1 4_1 5_1)_I$ is 12% of the assumed total rate and rises to 16% when allowance is made for transfer to unobserved rotational levels in $(3_1/2_1 4_1 5_1)_I$. In keeping with expectations based on conservation of nuclear spin, no evidence has been found for transitions involving odd changes in J. This phenomenon has been reported for certain perturbed levels of acetylene in the recent literature.[5–7] Fig. 4 shows the state-to-state rate coefficients plotted *versus* ΔE_{if}, the difference in energy between the initial and final rovibrational states. It is clear from examination of these data that, in RET transfer within the $(3_1/2_1 4_1 5_1)_{II}$ manifold, the $\Delta J = \pm 2$ transitions are strongly favoured. Indeed, they account for *ca.* 48% of the total relaxation. A similar propensity has been reported previously in related studies of state-to-state rotational energy transfer,[6,14] although it was not observed in previous work on the $(3_1/2_1 4_1 5_1)_{I,\,II}$ states.[11]

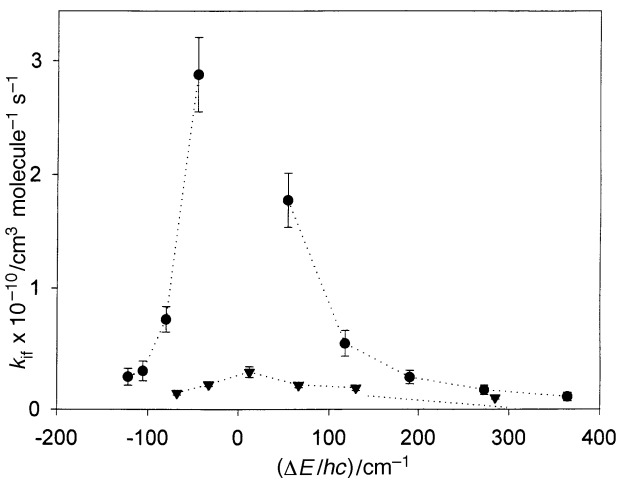

Fig. 4 State-to-state rate coefficients for self-relaxation from $(3_1/2_1 4_1 5_1)_{II}$, $J = 10$ displayed on a linear scale. The filled circles represent the rate coefficients for RET within the $(3_1/2_1 4_1 5_1)_{II}$ vibrational state, the filled triangles those for V–V intradyad transfer to specific rotational levels in the $(3_1/2_1 4_1 5_1)_I$ vibrational state. Errors shown correspond to two standard deviations.

(b) Rotational energy transfer in C_2H_2–C_2H_2 collisions: Comparisons with earlier work

Although our results are only directly comparable with those of Frost[11] who performed similar measurements on the same pair of Fermi dyad states, rates of rotational energy transfer are generally found to be independent of vibrational level, so the present data can be compared with a sizeable body of previous results on energy transfer in C_2H_2–C_2H_2 collisions. In making these comparisons we begin by considering the results for RET, *i.e.* for transfer from the initially prepared state $J_{II} = 10$, to other rotational levels within the $(3_1/2_1 4_1 5_1)_{II}$ state.

To make such comparisons, it is useful to compact the data using the empirical fitting laws that have frequently been employed for this purpose in the past. These comparisons are best made by applying detailed balance to the results for which $E_f < E_i$ (or those for which the reverse is true) so that the results for 'up' and 'down' transfers can be compared. We calculate rates for 'up' transfers using the equation:

$$k_{fi}/k_{if} = \{(2J_i + 1)/(2J_f + 1)\}\exp\{(E_f - E_i)/k_B T\} \quad (3)$$

to convert the measured rate coefficients for 'down' transfers into those for 'up' transfers.

The two simplest and most widely used fitting laws are the exponential gap law (EGL)

$$k_{if} = K_0 \exp(-\alpha\,|\,\Delta E_{if}\,|/k_B T) \quad (4a)$$

and the power gap law (PGL)

$$k_{if} = K'_0(|\,\Delta E_{if}\,|/B_v)^{-\delta} \quad (4b)$$

where B_v is the rotational constant of the molecule in a specific vibrational state. Although the state-to-state rate coefficients are generally expressed as functions of the energy gap, $\Delta E_{if} = (E_i - E_f)$, similar expressions in terms of ΔJ, the change in angular momentum, are also used. Our state-to-state rate coefficients are tested against the energy version of the EGL [eqn. (4a)] in Fig. 5.

The vibrational states in $C_2H_2(\tilde{X}\,^1\Sigma_g^+)$ for which state-to-state RET rate coefficients have been measured in previous studies are $(3_1/2_1 4_1 5_1)_I$,[11] 2_1,[12,13] $1_1 5_1$,[35] 3_3,[14] $2_4 4_3 5_3$.[15] (The notation used to identify these vibrational states is, of course, approximate as some states are heavily mixed.) In all these vibrational levels, the state-to-state rate coefficients for RET are seen to decrease with increasing ΔE_{if}. However, there appears to be a marked propensity for $\Delta J = \pm 2$ in certain states which is absent in others. In the cases where no such propensity has been observed, EGL fits have been used to correlate the rate coefficients. In the other cases, where a propensity for $\Delta J = \pm 2$ transitions has been noted, there is a problem of how best to describe the data. For the 3_3 manifold, Tobiason *et al.*[14] elected to use a combined exponential/power gap fitting law, which effectively skewed the fit upwards at low values of ΔE_{if}. These data have been re-analysed by Dolpheide *et al.*[13] producing an EGL fit for each value of ΔJ. Milce and Orr[6] have used two forms of the exponential gap law, treating the $\Delta J = \pm 2$ and the $\Delta J \geqslant 4$ data separately, with the parameter α for the $\Delta J = \pm 2$ fit constrained to the value found for the $\Delta J \geqslant 4$ fit. In view of the strong propensity that we have observed for $\Delta J = \pm 2$ transitions, we have adopted the approach of Milce and Orr and treated the $\Delta J = \pm 2$ data separately from the $\Delta J \geqslant 4$ data. The fits are shown in Fig. 5(a), each point being weighted according to its reciprocal error. The parameters derived from the fits are listed in Table 3.

Although Frost[11] populated $J = 12$ in the upper component of the $(3_1/2_1 4_1 5_1)$ Fermi dyad, rather than $J = 10$ in the lower component as in the present work, one might expect his results and ours to be directly comparable. However, there are discrepancies between the results of these two studies. Although the experimental technique used in the two cases was similar, the values for the UV intensity factors do not

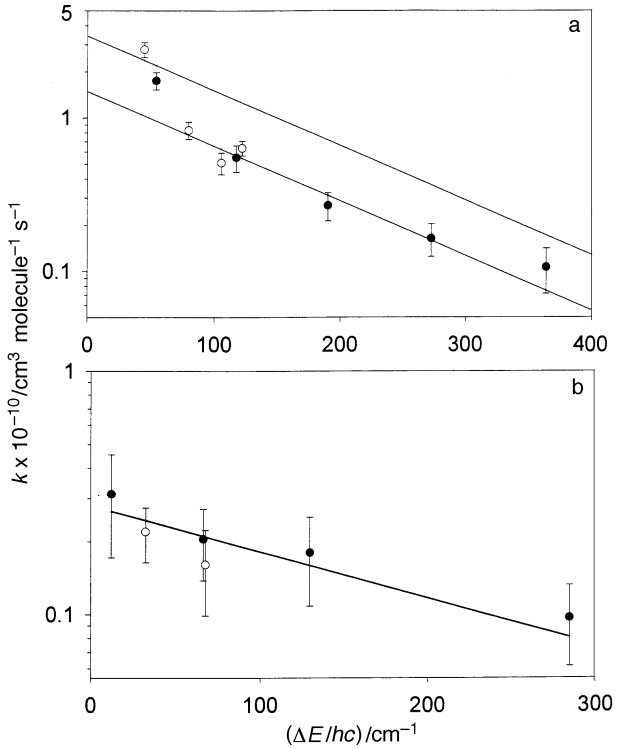

Fig. 5 Plot of rate coefficients for endoergic transfer in C_2H_2–C_2H_2 collisions, hollow symbols indicate rates obtained from the experimental data by the application of detailed balance. Plot (a) shows data for rotational energy transfer, plot (b) for intradyad V–V transfer. Lines shown in plot (a) are EGL fits to points with $\Delta J = \pm 2$ (upper) and with $\Delta J \geqslant 4$ (lower). A single EGL fit is shown in plot (b).

agree and the present observation of a strong propensity for $\Delta J = \pm 2$ transitions was not found in the earlier work.[11] The reason for these differences is not known, but we note that the observation of an 'additional' propensity for $\Delta J = \pm 2$ transitions (*i.e.* above that expected simply on the basis of the EGL) is reproduced in other work on strongly mixed vibrational levels in $C_2H_2(\tilde{X}\ ^1\Sigma_g^+)$.

Excluding Frost's work,[11] the only vibrational states in which no additional propensity for $\Delta J = \pm 2$ rotational transitions have been observed are 2_1 [12,13] and 1_15_1,[35] which are both of almost entirely unmixed vibrational character.[18] The vibrational states in which a marked propensity for $\Delta J = \pm 2$ transitions has been found in studies of RET are all of strongly mixed character: Thus $(3_3/1_12_13_14_2)$ and $(3_1/2_14_15_1)$ are coupled by Fermi resonance and $(2_44_35_3)$ is mixed with several other states, notably (2_13_3). It is also relevant to mention the work on RET in $N_2(v = 1)$,[36] as nitrogen has a similar rotational constant to acetylene but has, of course, a simple vibrational structure. In this case, there is no propensity for $\Delta J = \pm 2$ transitions above that expected on the basis of the EGL.

Table 3 EGL fit parameters associated with rotational state-to-state data from various vibrationally excited states in $C_2H_2(^1\tilde{X}_g^+)$

Vibrational level	EGL fit parameters[a] $K_0/10^{-10}$ cm^3 molecule^{-1} s^{-1}	α	Ref.
2_1	1.26 ± 0.46	1.16 ± 0.15	13
3_3, $\Delta J = 2$	3.25	2.92	13, 14
3_3, all ΔJ	1.96 ± 0.06	1.68 ± 0.03	14
$2_44_45_3$, $\Delta J = 2$	2.8	1.6[b]	6
$2_44_45_3$, $\Delta J \geqslant 4$	1.22	1.6	6
$(3_1/2_14_15_1)_\mathrm{I}$	2.5 ± 0.2	1.92 ± 0.17	11
$(3_1/2_14_15_1)_\mathrm{II}$, $\Delta J = 2$	3.4 ± 0.6	1.71[b]	This work
$(3_1/2_14_15_1)_\mathrm{II}$, $\Delta J \geqslant 4$	1.5 ± 0.25	1.71 ± 0.27	This work

[a] $k_\mathrm{if} = K_0 \exp(-\alpha|\Delta E_\mathrm{if}|/kT)$. [b] Constrained to this value, see text.

In the light of the above results, it seems that there may be some additional dynamical influence on rotational energy transfer in C_2H_2–C_2H_2 collisions when the excited molecules are in a perturbed vibrational state. The evidence for this proposition spans five vibrational bands of acetylene and a considerable range in energy. The role of long-range attractive forces in inducing RET has been recognised for collisions between dipolar molecules, such as HCN, leading to a strict $\Delta J = \pm 1$ selection rule.[37] For nonpolar molecules the situation is different and RET generally leads to a broad distribution of state-to-state rate coefficents over ΔJ. However, in view of the experimental observations of the state-to-state rate coefficients in acetylene self-collisions, it seems as if, at least for states of highly mixed vibrational character, attractive forces between the collision partners become important. The resultant propensity for $\Delta J = \pm 2$ transitions is consistent with long-range energy transfer under the influence of quadrupole–quadrupole interactions. It is noted that as the rate of rotational relaxation exceeds the Lennard–Jones collision rate,[38] attractive forces must play some role, although the total rate of rotational relaxation does not appear to vary according to the presence or not of the $\Delta J = \pm 2$ propensity.

(c) Rotationally specific intradyad transfer in C_2H_2–C_2H_2 collisions: Discussion

The state-to-state rate coefficients for transfer within the $(3_1/2_14_15_1)$ dyad are of particular interest, because of the unusual change in the composition of the rotational levels of both states with increasing J, which might be expected to affect the relative values of rotational state to rotational state rate coefficients.[39,40] Vander Auwera *et al.*[17] have shown that the dominant contribution to $(3_1/2_14_15_1)_\mathrm{I}$ is the zero order $|3_1\rangle$ state at values of $J < 11$, whereas for $J > 11$ the dominant contributor is $|2_1(4_15_1)^0\rangle$, whilst the reverse is true for $(3_1/2_14_15_1)_\mathrm{II}$.

The state-to-state rate coefficients determined in the present work for both RET and intradyad V–V transfer are given in Table 2 and their logarithms are plotted *versus* ΔE in Fig. 5. The values plotted are for transfer in the endoergic direction and include data calculated by applying detailed balance. It is observed that the rate coefficients for intradyad V–V transfer calculated from those for 'down' transfer from $J = 10$ fall marginally below those for 'up' transfer into $J = 10$, which agrees with the earlier observations,[11] although the effect is much less pronounced for the present set of rate coefficients. A more convincing example of such effects has been given by Milce and Orr[6] who populated the state labelled $2_44_35_3$ and observed transfer to this state from the coupled states $(2_13_3)_\mathrm{I,\ II}$. The latter vibrational states are strongly mixed and the resonance crossover at $J \approx 15$ is paralleled by a crossover in the values of the state-to-state rate coefficients. State-to-state vibrational energy transfer has also been measured for the $3_3 \rightarrow 1_12_13_14_2$ system of C_2H_2.[8] These earlier results are summarised in Table III of ref. 6. The parameters obtained from the EGL analysis of the present results which is shown in Fig. 5(b) are compared in Tables 3 and 4 with the results from previous investigations.

The work of Orr[39–41] has been valuable in developing an understanding of the factors which influence the rate of V–V transfer between levels mixed by Fermi resonance. He has emphasised the important role of the vibrational matrix element which, when only two zero order states $|v_a\rangle$ and $|v_b\rangle$ make significant contributions to the wavefunctions of the eigenstates, can be written as:

$$\langle \Psi_\mathrm{I}|V|\Psi_\mathrm{II}\rangle = \tfrac{1}{2}\sin 2\theta\{\langle v_b|V|v_b\rangle - \langle v_a|V|v_a\rangle\} + \cos 2\theta\langle v_a|V|v_b\rangle \quad (5)$$

Table 4 EGL fit parameters associated with intradyad V–V energy transfer

Initial-final state	EGL fit parameters[a] $K_0/10^{-10}$ cm^3 molecule^{-1} s^{-1}	α	Ref.
$(3_1/2_1 4_1 5_1)_I$–$(3_1/2_1 4_1 5_1)_{II}$	0.40 ± 0.12	1.7 ± 0.7	11
$(3_1/2_1 4_1 5_1)_{II}$–$(3_1/2_1 4_1 5_1)_I$	0.28 ± 0.03	0.91 ± 0.31	This work

[a] See note *a*, Table 3.

[see eqn. (8) in Part I]. In cases where the mixing is strong, $\theta \approx \pi/4$, the last term on the right-hand side of the equation is very small, and the magnitude of $\langle \Psi_I | V | \Psi_{II} \rangle$ depends on the relative magnitude of the diagonal terms $\langle v_b | V | v_b \rangle$ and $\langle v_a | V | v_a \rangle$.[41] Orr has shown[39] that the square of the vibrational matrix element for transfer between the states of the $(3_1/2_1 4_1 5_1)$ dyad of acetylene is $\leqslant 10^{-4}$ based on a 'breathing sphere' representation of the intermolecular potential. This result is clearly at odds with experimental observations, suggesting that anharmonic or long-range terms in the intermolecular potential may be important.[1,2,39]

Recognising that the high rate of V–V transfer between the states of the $(3_1/2_1 4_1 5_1)$ dyad in C_2H_2 means that the diagonal matrix elements must have significantly different values, Orr estimated the relative magnitude of these terms basing his calculation on Frost's experimental data[11] for the $\Delta J = \pm 2$ collisionally induced rates for RET and for V–V intradyad transfer from $J_i = 12$ in $(3_1/2_1 4_1 5_1)_{II}$. The basis of this treatment was to assume that the experimentally determined ratio k_{RET}/k_{V-V} is equal to the ratio of the square of the two matrix elements which differ only in the sign between the two diagonal elements. He found $\langle 2_1 4_1 5_1 | V | 2_1 4_1 5_1 \rangle / \langle 3_1 | V | 3_1 \rangle = 0.45 \pm 0.05$ although, as we have pointed out in Part I,[1] the reciprocal of this result *i.e.* 2.2, is equally valid. Moreover, this treatment neglects any difference in the form of the two rotational distributions: for RET within the initially excited vibrational state $(3_1/2_1 4_1 5_1)_{II}$ and for V–V transfer between states I and II. We have extended Orr's treatment to allow for this difference.

We start by expressing the collisional probabilities for transfer between particular rovibrational levels (P_{if}) as

$$P_{if} \propto |B\langle v_b | V | v_b \rangle + A\langle v_a | V | v_a \rangle|^2 f(J_f, J_i) \quad (6)$$

where A and B are of the same sign for RET within the same state but of opposite sign for V–V intradyad transfer. In this equation, the final, off-diagonal, term in eqn. (5) for the transition matrix element is omitted, and the J-dependence of the diagonal terms is included explicitly. Thus the magnitudes of the component diagonal matrix elements $\langle v_b | V | v_b \rangle$ and $\langle v_a | V | v_a \rangle$ are assumed to be J-independent. The J-dependent mixing coefficients determining the values of A and B are derived from the work of Vander Auwera *et al.*[17] (see Fig. 6 of ref. 17) together with the sign convention recommended by Orr.[39] They have been deposited as Supplementary Data. In terms of eqn. (5) and (6), $|v_a\rangle$ is $|3_1\rangle$, whilst $|v_b\rangle$ is $|2_1(4_1 5_1)^0\rangle + |2_1(4_1 5_1)^2\rangle$, assuming the reduced matrix elements associated with these σ ($k = 0$) and δ ($k = 2$) zero order states to be equivalent. A is therefore equal to the product of the mixing coefficients $a_i a_f$ and B is $b_i^\sigma b_f^\sigma + b_i^\delta b_f^\delta$ where the superscripts refer to the σ and δ states. The unusual, J-dependent, mixing of these states is therefore incorporated into this expression. The factors $f(J_f, J_i)$ are included to reproduce the distribution of the experimental state-to-state rate coefficients once the J-dependence of the matrix elements has been allowed for. A numerical procedure was followed, varying the relative values of $\langle v_b | V | v_b \rangle$ and $\langle v_a | V | v_a \rangle$ so that $\sum_{f,II} f(J_f, J_i) = \sum_{f,I} f(J_f, J_i)$ to fit the relative values of the experimental state-to-state rate coefficients. Solving eqn. (6) in this manner gave:

$$\langle 2_1 4_1 5_1 | V | 2_1 4_1 5_1 \rangle / \langle 3_1 | V | 3_1 \rangle = 0.37 \text{ or } 2.7 \quad (7)$$

where once again there is uncertainty as to which of the diagonal matrix elements is the larger.

Use of either of these values correctly predicts the ratio of the overall rates of RET to V–V intradyad transfer. This ratio is estimated from the simplified expression:

$$P_{V-V}/P_{RET} = \frac{|\langle 2_1 4_1 5_1 | V | 2_1 4_1 5_1 \rangle - \langle 3_1 | V | 3_1 \rangle|^2}{|\langle 2_1 4_1 5_1 | V | 2_1 4_1 5_1 \rangle + \langle 3_1 | V | 3_1 \rangle|^2} = 0.21 \quad (8)$$

In an effort to determine which of $\langle 2_1 4_1 5_1 | V | 2_1 4_1 5_1 \rangle$ and $\langle 3_1 | V | 3_1 \rangle$ is the larger, we have compared predictions of our model with features of both the present experimental results and those of Frost.[11] In particular, it is noticeable that our state-to-state rate coefficients for V–V intradyad transfer show a mild preference for transitions up *from* $J = 10$, rather than up *to* $J = 10$. Frost's data[11] show a similar but appreciably stronger trend. This propensity is consistent with evaluation of the J_f-dependent matrix elements with the ratio of the diagonal matrix elements given in eqn. (8) as 2.7 but not with the alternative value of 0.37. Therefore we tentatively conclude that the correct relationship between the diagonal matrix elements is $\langle 2_1 4_1 5_1 | V | 2_1 4_1 5_1 \rangle = 2.7 \langle 3_1 | V | 3_1 \rangle$. An EGL fit to these data yields parameters which are compared with the values before this allowance in Table 5.

Table 5 Comparison of EGL fit parameters before and after deperturbation

EGL α parameter[a]	RET ($\Delta J \geqslant 4$)	Intradyad V–V
Original	1.71 ± 0.27	0.91 ± 0.10
Deperturbed	1.79 ± 0.29	1.11 ± 0.21

[a] See note *a*, Table 3.

(d) Rotational energy transfer in collisions of C_2H_2 with Ar, He and H_2: Results

In order to determine state-to-state rate coefficients for transfer of C_2H_2 from $J = 10$ in the $(3_1/2_1 4_1 5_1)_{II}$ state in collisions with M = Ar, He and H_2, it was necessary to work with dilute mixtures of acetylene in M and to correct for the contribution of self-relaxation (see above). Using mixtures containing 10% acetylene ensured that the contribution of self-relaxation was less than *ca.* 30%. The total pressure of the mixture was chosen to be *ca.* 250 mTorr and LIF spectra were recorded at a time delay of *ca.* 100 ns.

Apart from the subtraction of factors allowing for self-relaxation, the experiments on C_2H_2–M mixtures were like those already described on samples of pure acetylene. This procedure gave the values of the state-to-state rate coefficients (k_{if}) for RET in collisions of $C_2H_2(3_1/2_1 4_1 5_1)_{II}$ with M = Ar, He and H_2 that are listed in Table 6. The rate coefficients (k_{fi}) for the reverse transfer, which have been calculated by applying detailed balance for the levels for which $E_f < E_i$, are also recorded in Table 6.

Attempts were also made to determine rate coefficients for rotationally resolved intradyad transfer from $(3_1/2_1 4_1 5_1)_{II}$, $J = 10$ induced by collisions with Ar, He and H_2. However, signal levels were found to be prohibitively low, confirming that these processes are slow. Part I [1] reports that the thermally averaged rate coefficient for intradyad V–V transfer with H_2 is $(8.6 \pm 0.5) \times 10^{-11}$ cm^3 molecule^{-1} s^{-1}, a factor of *ca.* 3 slower than the value reported for intradyad self-relaxation, and that the rates of transfer by Ar and He were much slower again. In the light of these figures, it is clear that intradyad transfer in mixtures containing 10% of C_2H_2 would

Table 6 State-to-state rate coefficients (units: 10^{-11} cm^3 molecule^{-1} s^{-1}) for the relaxation from the $(3_1/2_14_15_1)_{II}$, $J_{II} = 12$ level of $C_2H_2(^1\tilde{X}_g^+)$ by H_2, He and Ar

	H_2		He		Ar	
J_{II}	k_{if}	k_{fi}	k_{if}	k_{fi}	k_{if}	k_{fi}
2	1.1 ± 0.3	2.6 ± 0.7	1.6 ± 0.6	3.7 ± 1.5	2.2 ± 0.5	5.1 ± 1.2
4	1.3_5 ± 0.3	1.9 ± 0.5	2.8_5 ± 0.8	4.0 ± 1.1	3.3 ± 0.7	4.7_5 ± 1.0
6	5.9 ± 0.6	6.4 ± 0.7	6.0 ± 1.2	6.6 ± 1.3	6.7 ± 1.1	7.4 ± 1.3
8	12.1 ± 1.8	12.1 ± 1.1	9.8 ± 1.5	9.8 ± 1.5	9.4 ± 1.5	9.5 ± 1.5
10	—	—	—	—	—	—
12	11.0 ± 1.1	—	9.3 ± 1.7	—	9.5 ± 1.6	—
14	2.2 ± 0.5	—	3.6 ± 1.0	—	3.4 ± 0.7	—
16	1.7 ± 0.2	—	1.7 ± 0.5	—	2.2 ± 0.5	—
18	0.6 ± 0.15	—	1.2 ± 0.5	—	1.0 ± 0.2	—
Total	36.0	—	36.0	—	37.9	—

Cited errors represent relative error (2σ). No allowance is made for error in the total rate coefficient.

be both much slower than RET and also dominated by C_2H_2 collisions.

(e) Rotational energy transfer in collisions of C_2H_2 with Ar, He and H_2: Discussion

The present results for RET in collisions of C_2H_2 with Ar, He and H_2 represent the only extensive set of state-to-state rate coefficients that have been measured for collisions of acetylene with foreign gas collision partners. To examine these data, we have compared them with the results of two quantitative treatments: (i) the exponential gap and power gap laws, and (ii) the results of a simple classical model of collisions in which C_2H_2 is treated as a hard ellipsoid and the collision partner as a hard sphere. At the outset, we note that the additional propensity for $\Delta J = \pm 2$ transitions noted for C_2H_2–C_2H_2 collisions is absent in collisions of C_2H_2 with Ar, He and H_2.

The applicability of the EGL and PGL to the measured state-to-state rate coefficients is tested in Fig. 6. The fits are weighted to the reciprocal errors associated with each point and an estimate of the quality of the fits is made by calculating χ^2, the sum of the squares of the differences between the observed values of k_{if} and those expected on the basis of the EGL fit. Values of χ^2 are given in Table 7 along with the parameters appropriate to the two fitting laws. The EGL fits best as the mass of the collision partner increases whereas the reverse is true for the PGL. As far as the data are fitted by the EGL, it is clear that the parameters change with collision partner. In particular, as the mass of the collision partner increases, α falls substantially, reflecting the increasing breadth of the distribution of k_{if} with ΔE, which is easily observable from visual inspection of the state-to-state rate coefficients.

The apparent change from power gap to exponential gap behaviour as the collisional reduced mass increases is more difficult to rationalise. In general, power law behaviour has been observed over a wide range of systems comprising diatomic molecules and noble gases, with some exceptions to this for heavy molecule–light atom systems,[42] a trend which is opposite to that which we observe. According to the angular momentum transfer theory of McCaffery *et al.*,[43] high ΔJ transitions become disfavoured in collisions involving heavy molecules and light collision partners as a consequence of the need to conserve angular momentum in collisions. For light

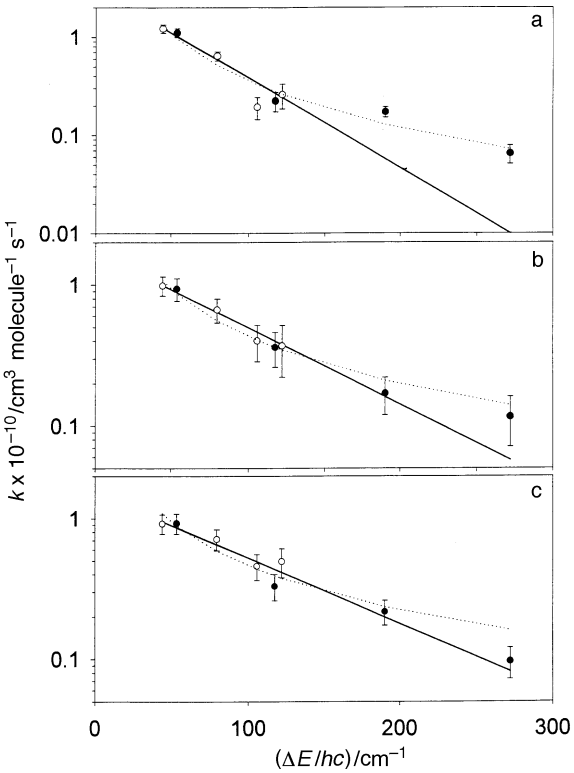

Fig. 6 Rotational state-to-state rate coefficients for endoergic transfer induced by collisions with (a) H_2, (b) He, and (c) Ar. Hollow symbols denote rate coefficients extracted by the application of detailed balance. EGL fits are shown by solid lines and PGL fits by dotted lines.

Table 7 EGL fit parameters asociated with the rate coefficients for RET within $(3_1/2_14_15_1)_{II}$ state induced by collisons with H_2, He and Ar

	EGL[a]			PGL[b]		
Collision partner	$K_0/10^{-10}$ cm^3 molecule^{-1} s^{-1}	α	χ^2	$K_0/10^{-10}$ cm^3 molecule^{-1} s^{-1}	δ	χ^2
H_2	3.2 ± 0.7[c]	4.4 ± 0.7	1.97	460 ± 335	1.6 ± 0.2	0.45
He	1.7_5 ± 0.15	2.6 ± 0.2	0.25	65 ± 24	1.1 ± 0.1	0.15
Ar	1.6 ± 0.15	2.2 ± 0.2	0.21	50 ± 28	1.0_5 ± 0.1	0.47

[a] Defined note *a*, Table 3. [b] Defined $k_{if} = K_0(|\Delta E_{if}|/kT)^{-\delta}$. [c] Cited errors correspond to a single standard deviation.

Table 8 Parameters for the 'ellipsoids of contact' used in the classical scattering calculations described in the text

System	Major axis (a)/Å	Minor axis (c)/Å	Ref.
C_2H_2–He	3.8	3.2	45(a)
C_2H_2–Ar	4.2	3.4	46(a)
C_2H_2–H_2	3.45	2.85	47

mass partners, the average value of orbital angular momentum at a particular temperature is less than for heavier collision partners. It seems unlikely that such considerations would be affected by the fact that C_2H_2 is polyatomic, since it is linear, or by the fact that it is in a vibrationally excited state.

Although total RET rates from specific vibrational levels of C_2H_2 in collisions with noble gases have been observed before,[10,15] there has been only one limited determination of rate coefficients for state-to-state transfer.[9] However, our results for C_2H_2–Ar can reasonably be compared with those for N_2–Ar for which a comparable set of state-to-state rate coefficients have been reported,[36] since these systems are similar in terms of collisional reduced mass, rotational constant and molecular symmetry. The variation of state-to-state rate coefficients, with $\Delta E(\Delta J)$ are similar in these two cases.

There have been a wide variety of theoretical approaches adopted for the calculation of cross-sections and rate coefficients for RET in molecular collisions, ranging from simple classical models to computations of quantum scattering on *ab initio* potential energy surfaces. Generally, it is assumed that the results will not depend, to any significant degree, on the vibrational state of the molecule so usually the internal coordinates are fixed at their equilibrium values and the potential energy surface is expressed as a function of three coordinates: the separation (r) of the centres of mass of the two colliding species and two angles representing the orientation between r and the main molecular axis.

We have performed classical calculations based on an extension of the treatment of Kreutz and Flynn[44] in which the 'hard' collision partners only interact, by impulsive repulsion, at an ellipsoidal surface whose dimensions are based on data for empirically based intermolecular potentials for these systems.[45–47] Such data, as well as high quality *ab initio* potentials, are available for both C_2H_2–He,[45] C_2H_2–Ar,[46] and C_2H_2–H_2.[47] We have chosen the values of the major (a) and minor (c) axes of each 'hard' ellipsoid to correspond to the values of r defining the onset of highly repulsive forces. These points are taken to be those at which the potential energy is half the average collision energy for collinear and perpendicular approach of M to C_2H_2. This approach yields the values of a and c which are given in Table 8.

Kreutz and Flynn[44] developed their model to treat the case of translationally 'hot' H atoms colliding with rotationally cold CO_2 at a defined collision energy.†† In the present work, the initial rotational state of C_2H_2 is defined (recall that $J_i = 10$ in the experiments) but the collision energies have a thermal distribution at 298 K. The latter circumstance is allowed for by choosing the collision energy for each individual calculation using a Monte Carlo method,[48] so that the thermal distribution is properly simulated in a full sample of 10^4 calculations.

The crux of the method[44] is to identify, for each 'trajectory', the point of impact on the ellipsoidal surface, then to calculate the resulting torque on the molecule resulting from the force acting perpendicular to the surface of the ellipsoid, and finally to calculate the final rotational angular momentum of the molecule by solving the appropriate equations for the conservation of angular momentum and total energy. Momentum parallel to the ellipsoidal surface is assumed to be conserved and the change in rotational momentum is necessarily restricted to that component in the plane containing the centre (of the molecule and the ellipsoid) and the vector ($\boldsymbol{n}$) perpendicular to the surface at the point-of-impact.

Monte Carlo methods[48] are adopted to select not only the collision energy/velocity, but also the impact parameter and angles defining the orientation of the molecule/ellipsoid at impact. The trajectory is assumed to follow a straight line up to the point-of-impact on the surface of the ellipsoid. The programme initially converts parameters, in particular the co-ordinates of the point-of-impact, expressed in space-fixed co-ordinates, chosen with respect to the direction of the linear momentum, into parameters in body-fixed co-ordinates expressed relative to the axes of the ellipsoid. This allows the 'effective' impact parameter (b_n)—which is the perpendicular distance from the centre of the ellipse to $\boldsymbol{n}$—and hence the torque to be calculated, and the conservation equations to be applied. The final value of the total rotational angular momentum (j') will not, of course, be a whole number so that it is necessary to employ the usual 'binning' procedures[48] whereby a result with $J - 1 \leqslant j' \leqslant J + 1$ where J is an even integer is assigned to the quantum level J. (Recall that from $J_i = 10$ only even values of J can be obtained by collisional energy transfer.)

Fig. 7 compares the results of the calculations with the experimentally determined state-to-state rate coefficients. The calculations reproduce the narrowing of the ΔJ distribution which is observed as the mass of the collision partner is reduced, an effect which presumably arises because of the smaller range of orbital momenta that is present for lower collisional reduced mass for a given collision energy or, on average, for a given temperature. In absolute terms, the calcu-

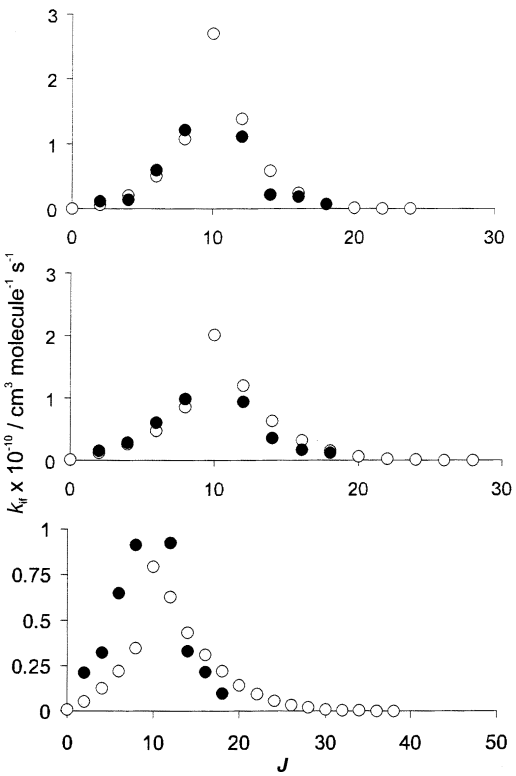

Fig. 7 Comparison of the experimental state-to-state rate coefficients for RET (●) induced by (a) H_2, (b) He, and (c) Ar with those calculated by the classical scattering model described in the text (○).

†† Kreutz and Flynn treated both rotational and vibrational inelasticity. The latter is not an issue in the present work and we consider only that part of Kreutz and Flynn's paper dealing with RET.

lated results for M = He and H_2 are in very good agreement with experiment but the rates of RET with M = Ar are underestimated.

The most likely explanation for the much poorer agreement in the case of C_2H_2–Ar collisions is that the model completely neglects attractive intermolecular forces. In the case of He and H_2, this approximation seems reasonable since the values of ε/k (the ratio of the intermolecular well-depth to the Boltzmann constant) are *ca.* 40 and 80 K, respectively; *i.e.* much smaller than kT at room temperature. For M = Ar, on the other hand, $\varepsilon/k \approx 150$ K.[49] It therefore seems that the collision dynamics will, in this case, be more affected by the attractive intermolecular forces which will, in particular, increase the overall collision cross-section.[49] As well as the poorer absolute agreement between the model calculations and experiment in the case of C_2H_2–Ar, it is also evident that the model seriously underestimates the rate coefficients for transitions in which $J_f < J_i$, whereas for $J_f > J_i$ the agreement is much better. Again this may be the result of neglecting attractive intermolecular forces which especially increase the number of collisions with low energy where transfer from the rotation of the molecule to the translational motion of the colliding species is most likely.

Clearly, it will be interesting to compare the results of more sophisticated scattering calculations using a full potential energy surface based on *ab initio* calculations with both the simple model calculations and the experimental results.

Summary and conclusions

Rate coefficients have been determined for rotationally resolved collisional processes within the $(3_1/2_14_15_1)$ Fermi dyad of $C_2H_2(\tilde{X}\,^1\Sigma_g^+)$. In the case of C_2H_2–C_2H_2 collisions, state-to-state rate coefficients are reported both for RET from $J = 10$ in the $(3_1/2_14_15_1)_{II}$ lower state of the dyad to other J levels within that state and for transfer from the same level $J_{II} = 10$ to rotational levels in the other state of the dyad, $(3_1/2_14_15_1)_I$. It is observed that RET accounts for *ca.* 76% of the total loss from $J_{II} = 10$, that transfer to the other dyad amounts to *ca.* 16%, the remainder being relaxation to vibrational levels lower than these dyad states. This result agrees well with previous measurements.[10,11] Within the $(3_1/2_14_15_1)_{II}$ state, RET in C_2H_2–C_2H_2 collisions shows a rather strong propensity for $\Delta J = \pm 2$ transitions which accounts for *ca.* 48% of the total relaxation, and it is suggested that such changes may be induced by long-range attractive forces arising from the interaction between quadrupole moments. An analysis of the present state-to-state data and that reported by Frost,[11] using the rovibrational eigenfunctions of Vander Auwera *et al.*[17] allows deperturbed values of the state-to-state rate coefficients to be derived. It is concluded that the facile nature of the intradyad transfer process is due to the dominance of the reduced diagonal matrix element associated with $|2_1(4_15_1)^0\rangle$ over that from $|3_1\rangle$ in the ratio *ca.* 2.7 : 1.

Results are reported for RET from $(3_1/2_14_15_1)_{II}$, $J_I = 10$ to other rotational levels within the same vibrational state in collisions with Ar, He and H_2. No propensity for $\Delta J = \pm 2$ transitions is observed for RET in these systems. The distribution of state-to-state rate coefficients with $\Delta E(\Delta J)$ becomes broader as the mass of the collision partner increases. The experimental results are compared with the exponential and power gap laws and with the results of simple classical scattering calculations in which only impulsive repulsive forces act between the collision partners. The agreement with the simple model calculations for C_2H_2–He and C_2H_2–H_2 collisions is rather good. The overall rate coefficient for RET is underestimated in the case of C_2H_2–Ar collisions and the distribution of state-to-state rate coefficients is significantly different from experiment. It is suggested that this is, at least in part, the result of neglecting long-range intermolecular forces which will increase the cross-section for core collisions.

We are grateful to EPSRC for a studentship (S.H.) and for a research grant in support of this work and thank Dr A. P. Milce for providing us with details of her analysis of the mixing in the $(3_14_1/2_14_25_1)_{I,II}$ dyad. We also acknowledge valuable discussions with F. F. Crim and B. J. Orr as well as a NATO Travel Grant which has enhanced our interaction with Professor Crim and his research group. Finally, we thank EOARD for support of our work on energy transfer under contract SPC-95-4030.

References

1 S. Henton, M. Islam and I. W. M. Smith, *J. Chem. Soc., Faraday Trans.*, 1998, **94**, 3207.
2 S. Henton, M. Islam and I. W. M. Smith, *Chem. Phys. Lett.*, 1998, **291**, 223.
3 M. J. Frost and I. W. M. Smith, *J. Phys. Chem.*, 1995, **99**, 1094.
4 B. L. Chadwick, A. P. Milce and B. J. Orr, *Chem. Phys.*, 1993, **175**, 113.
5 A. P. Milce and B. J. Orr, *J. Chem. Phys.*, 1996, **104**, 6423.
6 A. P. Milce and B. J. Orr, *J. Chem. Phys.*, 1997, **106**, 3592.
7 M. A. Payne, A. P. Milce, M. J. Frost and B. J. Orr, *Chem. Phys. Lett.*, 1997, **265**, 244.
8 J. D. Tobiason, A. L. Utz and F. F. Crim, *J. Chem. Phys.*, 1994, **101**, 1108.
9 J. D. Tobiason, M. D. Fritz and F. F. Crim, *J. Chem. Phys.*, 1994, **101**, 9642.
10 M. J. Frost and I. W. M. Smith, *Chem. Phys. Lett.*, 1992, **191**, 574.
11 M. J. Frost, *J. Chem. Phys.*, 1993, **98**, 8572.
12 R. Dopheide, W. B. Gao and H. Zacharias, *Chem. Phys. Lett.*, 1991, **182**, 21.
13 R. Dopheide, W. Cronrath and H. Zacharias, *J. Chem. Phys.*, 1994, **101**, 5804.
14 J. D. Tobiason, A. L. Utz and F. F. Crim, *J. Chem. Phys.*, 1992, **97**, 7437.
15 A. L. Utz, J. D. Tobiason, E. Carrasquillo, M. D. Fritz and F. F. Crim, *J. Chem. Phys.*, 1992, **97**, 389.
16 B. C. Smith and J. S. Winn, *J. Chem. Phys.*, 1988, **89**, 4638.
17 J. Vander Auwera, D. Hurtmans, M. Carleer and M. Herman, *J. Mol. Spectrosc.*, 1993, **15**, 337.
18 M. A. Temsamani and M. Herman, *J. Chem. Phys.*, 1995, **102**, 6371.
19 (*a*) A. Campargue, L. Biennier and M. Herman, *Mol. Phys.*, 1998, **93**, 457; (*b*) A. Campargue, M. A. Temsamani and M. Herman, *Mol. Phys.*, 1998, **93**, 793; (*c*) S. F. Yang, L. Biennier, A. Campargue, M. A. Temsamani and M. Herman, *Mol. Phys.*, 1998, **93**, 807.
20 M. A. Temsamani, M. Herman, S. A. B. Solina, J. P. O'Brien and R. W. Field, *J. Chem. Phys.*, 1996, **105**, 11 357.
21 (*a*) A. L. Utz, J. D. Tobiason, E. Carrasquillo, L. J. Sanders and F. F. Crim, *J. Chem. Phys.*, 1993, **98**, 2742; (*b*) J. D. Tobiason, A. L. Utz and F. F. Crim, *J. Chem. Phys.*, 1993, **99**, 928, (*c*) J. D. Tobiason, A. L. Utz, E. L. Sibert, III and F. F. Crim, *J. Chem. Phys.*, 1993, **99**, 5762.
22 T. A. Brunner, N. Smith, A. W. Karp and D. E. Pritchard, *J. Chem. Phys.*, 1981, **74**, 3324.
23 C. Ottinger and M. Schroder, *J. Phys. B*, 1980, **13**, 4163.
24 B. E. Wilcomb and P. J. Dagdigian, *J. Chem. Phys.*, 1977, **67**, 3829.
25 P. J. Dagdigian and B. E. Wilcomb, *J. Chem. Phys.*, 1980, **72**, 6462.
26 N. Smith, T. A. Brunner and D. E. Pritchard, *J. Chem. Phys.*, 1981, **74**, 467.
27 (*a*) M. Islam, I. W. M. Smith and J. W. Wiebrecht, *J. Phys. Chem.*, 1994, **98**, 9285; (*b*) M. Islam, I. W. M. Smith and J. W. Wiebrecht, *J. Chem. Phys.*, 1995, **103**, 9676.
28 (*a*) P. L. James, I. R. Sims, I. W. M. Smith, *Chem. Phys. Lett.*, 1997, **272**, 412; (*b*) P. L. James, I. R. Sims, I. W. M. Smith, M. H. Alexander and M. Yang, *J. Chem. Phys.*, 1998, in press.
29 (*a*) T. Oka, *J. Chem. Phys.*, 1967, **47**, 4852; (*b*) T. Oka, *J. Chem. Phys.*, 1968, **49**, 3135; (*c*) T. Oka, *J. Chem. Phys.*, 1973, **9**, 127.
30 R. M. Lees and T. Oka, *J. Chem. Phys.*, 1969, **51**, 3027.
32 P. J. Seibt, *J. Chem. Phys.*, 1972, **57**, 1343.
32 J. B. Cohen and E. B. Wilson, Jr., *J. Chem. Phys.*, 1973, **58**, 442.
33 J. K. G. Watson, M. Herman, J. C. Van Craen and R. Colin, *J. Mol. Spectrosc.*, 1982, **95**, 101.

34 I. W. M. Smith and J. F. Warr, *Chem. Phys. Lett*., 1990, **173**, 70.
35 A. S. Pine and J. P. Looney, *J. Chem. Phys*., 1990, **93**, 6942.
36 G. O. Sitz and R. L. Farrow, *J. Chem. Phys*., 1990, **93**, 7883.
37 T. Oka, *J. Chem. Phys*., 1968, **48**, 4919.
38 The Lennard-Jones collision rate for C_2H_2–C_2H_2 collisions is given as 16.0 ms^{-1} $Torr^{-1}$ ($\equiv 4.9 \times 10^{-10}$ cm^3 $molecule^{-1}$ s^{-1}) in accord with previous workers.[5,9]
39 B. J. Orr, *Chem. Phys*., 1995, **190**, 261.
40 B. J. Orr in *Advances in Chemical Kinetics and Dynamics. Vol.2: Vibrational Energy Transfer involving Large and Small Molecules*, ed. J. R. Barker, JAI Press, 1995, p. 21.
41 B. J. Orr and I. W. M. Smith, *J. Phys. Chem*., 1987, **91**, 6106.
42 S. L. Dexheimer, M. Durand, T. A. Brunner and D. E. Pritchard, *J. Chem. Phys*., 1982, **76**, 4996.
43 A. J. McCaffery, Z. T. Alwahabi, M. A. Osborne and C. J. Williams, *J. Chem. Phys*., 1993, **98**, 4586; M. A. Osborne and A. J. McCaffery, *J. Chem. Phys*., 1994, **101**, 5604; M. A. Osborne, A. J. Marks and A. J. McCaffery, *J. Phys. Chem*., 1996, **100**, 3888.
44 T. G. Kruetz and G. W. Flynn, *J. Chem. Phys*., 1990, **93**, 452.
45 (*a*) L. J. Danielson, M. Keil and P. J. Dunlop, *J. Chem. Phys*., 1988, **88**, 4218; (*b*) R. Moszynski, P. E. S. Wormer and A. van der Avoird, *J. Chem. Phys*., 1995, **102**, 8385.
46 (*a*) A. E. Thornley and J. M. Hutson, *Chem. Phys. Lett*., 1992, **198**, 1; (*b*) R. J. Bemish, P. A. Block, L. G. Pederson, W. Yang and R. E. Miller, *J. Chem. Phys*., 1993, **99**, 8585; (*c*) M. Yang and R. O. Watts, *J. Chem. Phys*., 1994, **101**, 8784; (*d*) M. Yang, M. H. Alexander, H-J. Werner and R. J. Bemish, *J. Chem. Phys*., 1996, **105**, 10462.
47 M. Yang and R. O. Watts, *J. Chem. Phys*., 1994, **100**, 3582.
48 I. W. M. Smith, *Kinetics and Dynamics of Elementary Gas Reactions*, Butterworths, London, 1980.
49 J. O. Hirschfelder, C. F. Curtiss and R. B. Bird, *Molecular Theory of Gases and Liquids*, Wiley, New York, 1954.

Paper 8/05898I